

Quantum reflection of bright solitary matter-waves from a narrow attractive potential

A. L. Marchant,¹ T. P. Billam,¹ M. M. H. Yu,¹ A. Rakonjac,¹
J. L. Helm,¹ J. Polo,² C. Weiss,¹ S. A. Gardiner,¹ and S. L. Cornish^{1,*}

¹Joint Quantum Centre (JQC) Durham-Newcastle, Department of Physics,
Durham University, Durham DH1 3LE, United Kingdom

²Department de Física, Universitat Autònoma de Barcelona, E-08193 Bellaterra, Spain

(Dated: September 12, 2018)

We report the observation of quantum reflection from a narrow, attractive, potential using bright solitary matter-waves formed from a ^{85}Rb Bose–Einstein condensate. We create narrow potentials using a tightly focused, red-detuned laser beam, and observe reflection of up to 25% of the atoms, along with the trapping of atoms at the position of the beam. We show that the observed reflected fraction is much larger than theoretical predictions for a narrow Gaussian potential well; a more detailed model of bright soliton propagation, accounting for the generic presence of small subsidiary intensity maxima in the red-detuned beam, suggests that these small intensity maxima are the cause of this enhanced reflection.

PACS numbers: 03.75.Lm, 03.75.-b, 03.75.Kk

Solitons are non-dispersive and self-localised wave solutions that arise when nonlinear interactions are sufficient to overcome the wavepacket dispersion. Since the first observations in shallow water [1], extensive studies of such solitary wave solutions have been carried out in a diverse range of fields, including nonlinear optics and optical fibers [2–4], plasma physics [5] and magnetism [6]. In the context of quantum gases, quasi-one-dimensional (1D) Bose–Einstein condensates (BECs) may be well described by the homogeneous 1D Gross-Pitaevskii equation (GPE), a nonlinear Schrödinger equation that manifests exact bright soliton solutions for attractive interatomic interactions, taking the form of localised density maxima [7]. Experimentally, a quasi-1D limit is approached by confining the condensate in a highly elongated trap with tight radial confinement. While such traps typically also feature weak axial confinement, precluding mathematically exact soliton solutions, the resulting solitary wave solutions retain many characteristics of the ideal soliton [8–10]. Previous experimental work has realized both single and multiple bright solitary matter-waves using ^7Li atoms [11–13] and ^{85}Rb atoms [14–16], stimulating intense theoretical interest (see [10] and references therein).

Scattering of bright solitary matter waves from narrow *repulsive* potential barriers has been extensively studied theoretically in the context of matter-wave interferometry [17–22]. The nature of the scattering depends crucially on the center-of-mass kinetic energy of the solitary wave relative to the modulus of its ground state energy. For high kinetic energies the barrier can act as a beam splitter; the two resulting solitary waves can then be recombined to form an interferometer [17], with the outcome of the recombination depending strongly on their relative phase [23] (as recently experimentally demonstrated [24]). For low kinetic energies, the scattering of the matter-wave soliton from the barrier can produce quantum superposition states [25–27]. Previous theoretical studies have also addressed the scattering of bright solitary waves from narrow *attractive* potential wells, where the possibility exists for the bright solitary wave to undergo quantum reflection.

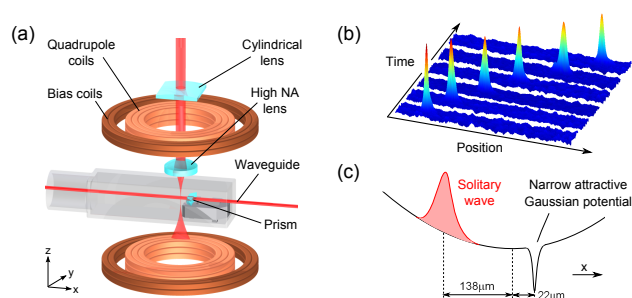


FIG. 1. (Color online) (a) Experimental setup. Atoms are cooled in a crossed optical dipole trap (not shown), and then transferred into an optical waveguide. Additional axial confinement is provided by magnetic quadrupole and bias fields. The narrow attractive potential is formed using a high numerical aperture (NA) lens to produce a light sheet, tightly focussed in the x direction. (b) Absorption images of solitary wave propagation in the optical waveguide. (c) Schematic showing the position of the narrow attractive potential, relative to the trap center and the initial position of the solitary wave.

Depending on the parameter regime, significant quantum reflection has been predicted for low energy solitons [28], and significant resonant trapping when the attractive potential is capable of supporting a number of bound states [29].

In this Letter, we report the observation of splitting and quantum reflection of a bright solitary matter-wave from a narrow, attractive potential formed from a tightly focused, red-detuned laser beam. We investigate how the fraction of atoms reflected varies with the depth of the attractive potential, and observe atoms trapped at the position of the well. Surprisingly, we measure much greater reflected fractions than can be explained by theoretical predictions for a Gaussian potential well. We address this discrepancy via extensive theoretical modeling using the GPE, providing strong evidence that the presence of small subsidiary diffraction maxima in the red-detuned beam, creating a multiple-well structure, is the main source of the enhanced reflection. While small subsidiary diffraction maxima are generically expected in tightly-focused

beams, our experiment is unusual in that they cause qualitative changes in behavior. Our results suggest that carefully engineered attractive multi-well potentials may make robust beamsplitters for solitary wave interferometry.

In this work we create stable ^{85}Rb condensates using the method described in [30]. We use the broad Feshbach resonance at 155 G between atoms in the $F = 2, m_F = -2$ state [31] to tune the scattering length to positive values, avoiding the large negative background scattering length and the associated collapse instability [32–34]. Our setup uses a levitated crossed optical dipole trap [35] [36], providing independent control of the trapping frequencies (dominated by the optical confinement) and the magnetic bias which is used to tune the scattering length (with a sensitivity $\sim 40 a_0 \text{ G}^{-1}$ around the zero crossing of the Feshbach resonance). We produce nearly pure condensates of up to 4×10^4 atoms at a scattering length of $a_s \approx 200 a_0$ in an almost spherical trapping geometry, $\omega_{x,y,z} = 2\pi \times \{30(1), 30(1), 42(2)\} \text{ Hz}$. The condensate number is reduced to ~ 6000 atoms by further evaporation to facilitate solitary wave production.

We form a bright solitary wave by loading the BEC into an optical waveguide created by an additional dipole trapping beam [15] as shown in Fig. 1(a). We first ramp the scattering length to a small positive value, $\sim 5 a_0$, over 50 ms. We then simultaneously ramp the crossed dipole beams off and the waveguide beam on in 250 ms. At the same time, we increase the magnetic field gradient to exactly levitate the atoms, and ramp the bias field to give a scattering length of $a_s = -7 a_0$. This value of a_s minimises the dispersion of the condensate as it travels along the waveguide, see Fig. 1(b). After the loading is completed the BEC is confined radially in the waveguide beam but is free to propagate along the axial direction. The combination of the magnetic field gradient, B'_z , and the magnetic bias field, B_z , produces a weak harmonic potential in the axial direction, given by $\omega_x = 1/2 \sqrt{\mu B_z'^2 / m B_z}$, where μ is the magnetic moment of the atoms, and m their mass [37]. This magnetic potential dominates the weak ($< 0.1 \text{ Hz}$) optical potential of the waveguide in the axial direction yielding overall trapping frequencies of $\omega_{x,y,z} = 2\pi \times \{1.15(5), 18.2(5), 18.2(5)\} \text{ Hz}$. By carefully positioning the magnetic potential minimum with respect to the crossed dipole trap we are able to control the motion of the atoms in the waveguide.

We produce a narrow attractive potential well using $\lambda = 852 \text{ nm}$ light, focussed to form a light sheet and determine the beam waists of $w_x = 1.9(2) \mu\text{m}$ and $w_y = 570(40) \mu\text{m}$ via parametric heating of atoms trapped at the focus of the beam. The potential well is precisely aligned with respect to the waveguide in the vertical direction by mounting the final lens in a threaded mount with a pitch of $1.4 \mu\text{m deg}^{-1}$. We position the potential well $\sim 22 \mu\text{m}$ from the minimum of the axial waveguide potential and release the solitary waves from the crossed dipole trap situated $\sim 160 \mu\text{m}$ away from the well [as shown in Fig. 1(c)], giving an incident velocity of $\sim 1 \text{ mm s}^{-1}$. At full power we obtain a maximum well depth of $1 \mu\text{K} \times k_B$.

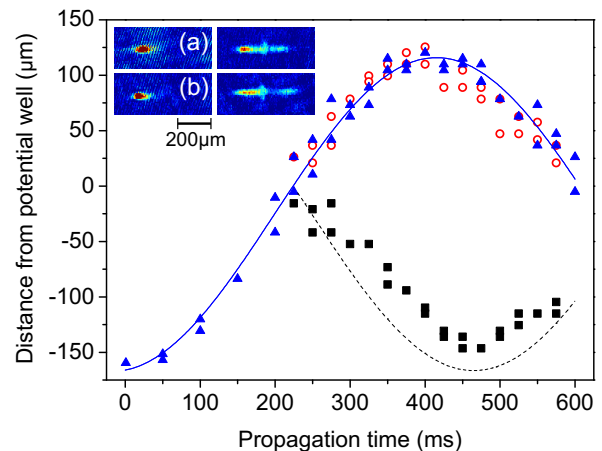


FIG. 2. (Color online) Solitary wave position as a function of time. In the absence of the well (blue triangles) the atoms oscillate in the waveguide. With the well present the solitary wave splits, with atoms being both transmitted (red circles) and reflected (black squares). Lines indicate classical trajectories for free propagation (solid) and elastic reflection (dashed). Inset: False colour images taken at (a) 375 ms and (b) 475 ms with the well present (right) and absent (left).

In our initial experiment we set the potential well depth to its maximum value, release a solitary wave into the waveguide, and track its position by imaging multiple instances of the same experimental sequence at different times after release. Once the solitary wave reaches the well, we observe a splitting of the wavepacket and identify three distinct resulting fragments: atoms transmitted, reflected, and confined at the potential well. We are able to track the center-of-mass positions of both the transmitted and reflected atomic clouds, as shown in Fig. 2. The majority of atoms in the solitary wave are transmitted (red circles), following the same trajectory as in the freely propagating case (blue triangles), undergoing harmonic motion in the waveguide (solid line). Around 5–10% of the atoms are confined close to the well. The remainder of the atoms ($\sim 25\%$) reflect from the narrow potential well and propagate in the opposite direction to the transmitted component. The turning point of the reflected atoms occurs $\sim 50 \text{ ms}$ later than for the transmitted atoms, due to the offset of the well position from the trap center. This turning point is $\sim 20 \mu\text{m}$ short of the release position, suggesting some energy is lost during the splitting process. For comparison, the trajectory of an elastic collision is shown by the dashed line in Fig. 2.

To explore the effect of the potential well depth relative to the energy of the incoming solitary wave we vary the power of the 852 nm beam, while keeping all other parameters constant. The solitary wave is split and the resulting fragments allowed to spatially separate before they are imaged, 475 ms after release. To calculate the reflection probability, we define three fixed regions of the absorption images: transmitted (T), confined (C), and reflected (R), as shown in the inset of Fig. 3(a). Taking the sum of the pixel values in each of these regions

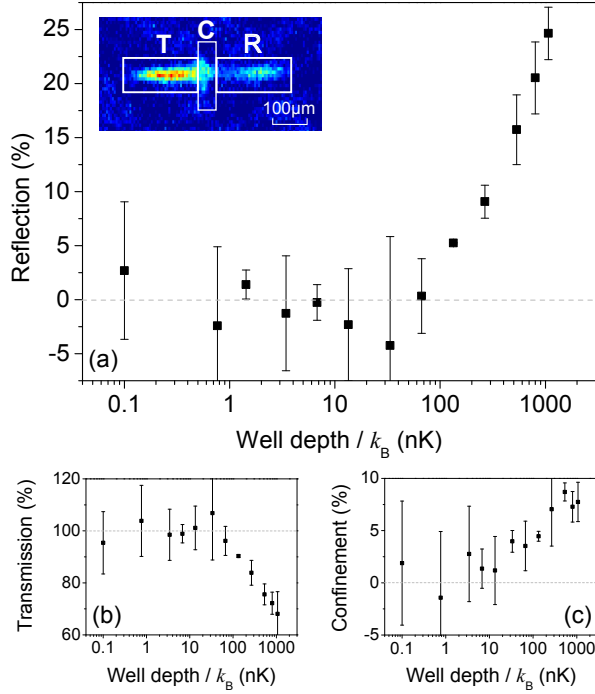


FIG. 3. (Color online) The percentage (a) reflection (R), (b) transmission (T), and (c) confinement (C), of atoms as a function of well depth for an incident solitary wave with a velocity of 1 mm s^{-1} . These percentages are determined using regions defined in the inset of (a). See text for details.

we define the reflection probability as $R/(R + C + T) \times 100\%$ (values for the transmitted and confined parts are calculated similarly) [38]. We find there is no observable reflection from the narrow potential well for trap depths $< 100 \text{ nK}$. Above this threshold, the probability of reflection increases sharply [see Fig. 3 (a)], and the number of atoms transmitted drops correspondingly [Fig. 3 (b)]. For a trap depth of $1 \mu\text{K} \times k_B$, we observe a reflection of $\sim 25\%$. The number of atoms confined at the position of the well also increases with increasing well depth, as shown in Fig. 3 (c).

Intriguingly, the observed coefficient of reflection [Fig. 3(a)] is too large to be explained in terms of quantum reflection from a Gaussian potential well,

$$V_G(x) = -V_0 \exp(-2x^2/\ell^2), \quad (1)$$

where $V_0 > 0$ and $\ell = 1.9 \mu\text{m}$. A simple approximate argument for this comes from the analytic formula for the single-particle reflection coefficient for the similar potential $V(x) = -V_0/\cosh^2(x/d)$ (choosing $d \approx \ell/1.6$) [39]

$$R = \frac{\cos^2\left(\pi\sqrt{1/4 + 2mV_0d^2/\hbar^2}\right)}{\sinh^2(\pi kd) + \cos^2\left(\pi\sqrt{1/4 + 2mV_0d^2/\hbar^2}\right)}, \quad (2)$$

where k is the wavevector of the incoming plane wave. Since $\cos^2(x) \leq 1$ for all real arguments x , this approximation shows that for $\ell = 1.9 \mu\text{m}$ a small incoming velocity (small k) is nec-

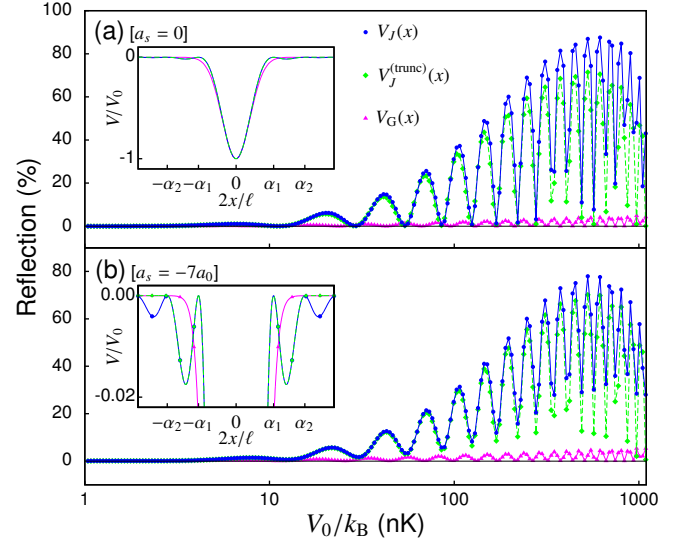


FIG. 4. (Color online) Reflection coefficients as a function of potential well depth for non-interacting wavepackets (a) and bright solitary waves (b) in a 1D GPE model. Results are shown for a Gaussian potential well with a single potential minimum [$V_G(x)$], and for diffraction pattern [$V_J(x)$] and truncated diffraction pattern [$V_J^{(\text{trunc})}(x)$] potentials with subsidiary minima (see insets).

essary to observe any reflection, *regardless of the well depth* V_0 . For velocities $v \approx 1 \text{ mm s}^{-1}$, as realized in the experiment, this approximation predicts negligible reflection.

This lack of substantial reflection from the Gaussian potential $V_G(x)$ [Eq. (1)] is confirmed by detailed numerical simulations of a quasi-one-dimensional GPE

$$i\hbar \frac{\partial \psi(x, t)}{\partial t} = \left[\frac{-\hbar^2}{2m} \frac{\partial^2}{\partial x^2} + V(x) + U(x, t) + g_{1D} |\psi(x, t)|^2 \right] \psi(x, t), \quad (3)$$

where $U(x, t)$ represents the time-dependent background potential (see lower curves in Fig. 4). We model the latter as

$$U(x, t) = \frac{1}{2} m \left[\omega_{x_1}(t)^2 (x - x_1)^2 + \omega_{x_2}(t)^2 (x - x_2)^2 \right], \quad (4)$$

where $x_1 = -160 \mu\text{m}$ ($x_2 = -22 \mu\text{m}$) represents the location of the minimum of the dipole (waveguide) potential in x , see Fig. 1 (c). The trap frequencies for these potentials are ramped linearly over the first $\tau = 250 \text{ ms}$: $\omega_{x_1}(t) = \max\{2\pi\nu_1(\tau - t)/\tau, 0\}$ and $\omega_{x_2}(t) = \min\{2\pi\nu_2 t/\tau, 2\pi\nu_2\}$, for $\nu_1 = 30 \text{ Hz}$ and $\nu_2 = 1.15 \text{ Hz}$. The (static) potential well $V(x)$ is centered on $x = 0$ in these coordinates, and the atoms move towards positive x . The nonlinearity $g_{1D} = 4\pi N a_s \hbar v_\perp$, where we take $N = 6000$ and $v_\perp = 18.2 \text{ Hz}$. We work with $\psi(x, t)$ normalized to unity, and initialize the simulation with $\psi(x, t)$ in the ground state of the system for potential $U(x, t = 0)$. In agreement with the approximate formula [Eq. (2)], these simulations confirm that only very weak reflection ($\lesssim 4\%$) is expected from the Gaussian potential $V_G(x)$, both for non-interacting wavepackets [Fig. 4(a), $a_s = 0$], and for bright solitary waves [Fig. 4(b), $a_s = -7a_0$]. We have confirmed that

the amount of reflection is not significantly changed by the use of a fully three-dimensional GPE model, the inclusion of noise in the initial wavepacket, or both of these extensions.

To qualitatively explain the surprisingly large observed reflections we consider the effects of subsidiary diffraction maxima in the optical intensity, which occur generically in focusing optical configurations [40]. Since these are generally much less intense than the primary maximum, they are typically ignored when calculating optical potentials in BEC experiments. However, in the context of our experiment, the *narrow* nature of the subsidiary maxima is potentially significant; at least when considered in isolation, they are able to produce larger reflection than the primary maximum [see Eq. (2)]. Also, the presence of multiple potential wells can itself enhance reflection; this is seen, for example, in Bragg reflection of BECs from a multiple-well lattice [41] (although in our case the rapid variation in well depths precludes a similar analysis).

While the exact structure of the subsidiary diffraction maxima in the red-detuned beam is not precisely known in our experiment, as a generic model we consider the potential due to the intensity pattern of Fraunhofer diffraction from an aperture [40]

$$V_J(x) = -V_0 \left[\frac{\ell}{x} J_1 \left(\frac{2x}{\ell} \right) \right]^2, \quad (5)$$

and the same potential truncated after the first subsidiary maxima;

$$V_J^{(\text{trunc})}(x) = \begin{cases} V_J(x) & |2x/\ell| < \alpha_2, \\ 0 & |2x/\ell| \geq \alpha_2, \end{cases}, \quad (6)$$

where α_2 is the second positive zero of the Bessel function $J_1(x)$. As shown in Fig. 4 (inset) these potentials have a similar central minimum to $V_G(x)$, but also one [$V_J^{(\text{trunc})}(x)$] or a decaying series [$V_J(x)$] of subsidiary minima. The results of 1D GPE simulations for both noninteracting wavepackets [Fig. 4(a), $a_s = 0$] and for bright solitary waves [Fig. 4(b), $a_s = -7a_0$] show that the reflection is greatly enhanced for both of these potentials compared to $V_G(x)$, for the range of well depths used in the experiment. The presence of subsidiary diffraction maxima in the beam producing the potential well thus provides a plausible explanation for the non-zero reflection probabilities observed in the experiment. The similarity of the results for $V_J(x)$ and $V_J^{(\text{trunc})}(x)$ indicate that the oscillatory structure of the reflection coefficient is primarily a transmission resonance effect, attributable to the three-well potential composed of the main beam maximum and the largest two subsidiary diffraction maxima.

There are quantitative differences between the experimental data [Fig. 3(a)] and this generic model; in particular, the model exhibits negligible ($< 1\%$) confinement, and oscillatory structure. We have excluded small shot-to-shot changes in the incoming soliton velocity due to small ($\sim \pm 5 \mu\text{m}$) shifts in the alignment of the experimental potentials as an explana-

tion for the lack of oscillations in the experiment; changing the initial displacement of the soliton by up to $\pm 5 \mu\text{m}$ in the model leads to a negligible change in reflection coefficient. We suspect that these remaining differences may arise from effects not captured by our one-dimensional Gross-Pitaevskii model, such as the exact structure of the potential well (possibly including time-dependent fluctuations), three-dimensional effects, and finite-temperature effects.

In summary, we have observed quantum reflection of a bright solitary matter-wave from a narrow, attractive potential, formed by a tightly focused laser beam. Reflection probabilities of up to 25% are measured, with the remaining atoms either transmitted or trapped at the position of the potential well. Modeling of the system suggests that the exact spatial form of the potential well is crucial in determining the amount of reflection observed, with the presence of multiple optical diffraction maxima, rather than a single Gaussian maximum, playing an essential role. These results indicate that carefully engineered attractive multi-well potentials could be developed as robust beamsplitters for use in solitary wave interferometry. In future work we plan to replace the focused laser beam with a room-temperature super-polished glass prism (shown in Fig. 1), allowing us to explore quantum reflection due to the attractive Casimir-Polder potential [42].

The data presented in this paper are freely available to download [43].

We thank Ifan Hughes and Matthew Jones for useful discussions. We acknowledge the UK Engineering and Physical Sciences Research Council (Grant No. EP/L010844/1, Grant No. EP/K030558/1) for funding. T.P.B. acknowledges financial support from the John Templeton Foundation via the Durham Emergence Project (<http://www.dur.ac.uk/emergence>). J.P. acknowledges financial support from the FPI grant BES-2012-053447 and the mobility grant EEBB-I-14-08515, associated to the project FIS2014-57460-P, and from the Catalan government under the SGR 2014-1639 grant.

* s.l.cornish@durham.ac.uk

- [1] Russell, J. Scott, in *Report of the Fourteenth Meeting of the British Association for the Advancement of Science* (John Murray, 1845) p. 311.
- [2] L. F. Mollenauer, R. H. Stolen, and J. P. Gordon, *Phys. Rev. Lett.* **45**, 1095 (1980).
- [3] Y. V. Kartashov, B. A. Malomed, and L. Torner, *Rev. Mod. Phys.* **83**, 247 (2011).
- [4] Y. S. Kivshar and G. Agrawal, *Optical Solitons: From Fibers to Photonic Crystals* (Elsevier Science, 2003).
- [5] K. Stasiewicz, P. K. Shukla, G. Gustafsson, S. Buchert, B. Lavraud, B. Thidé, and Z. Klos, *Phys. Rev. Lett.* **90**, 085002 (2003).
- [6] Y. Togawa, Y. Kousaka, S. Nishihara, K. Inoue, J. Akimitsu, A. S. Ovchinnikov, and J. Kishine, *Phys. Rev. Lett.* **111**, 197204 (2013).
- [7] P. Kevrekidis, D. Frantzeskakis, and R. Carretero-González, *Emergent Nonlinear Phenomena in Bose-Einstein Condensates*

- (Springer, 2008).
- [8] L. D. Carr and Y. Castin, *Phys. Rev. A* **66**, 063602 (2002).
- [9] T. P. Billam, S. A. Wrathmall, and S. A. Gardiner, *Phys. Rev. A* **85**, 013627 (2012).
- [10] T. P. Billam, A. L. Marchant, S. L. Cornish, S. A. Gardiner, and N. G. Parker, in *Spontaneous Symmetry Breaking, Self-Trapping, and Josephson Oscillations*, Progress in Optical Science and Photonics, Vol. 1, edited by B. A. Malomed (Springer, 2013) p. 403.
- [11] L. Khaykovich, F. Schreck, G. Ferrari, T. Bourdel, J. Cubizolles, L. D. Carr, Y. Castin, and C. Salomon, *Science* **296**, 1290 (2002).
- [12] K. E. Strecker, G. B. Partridge, A. G. Truscott, and R. G. Hulet, *Nature (London)* **417**, 150 (2002).
- [13] P. Medley, M. A. Minar, N. C. Cizek, D. Berryrieser, and M. A. Kasevich, *Phys. Rev. Lett.* **112**, 060401 (2014).
- [14] S. L. Cornish, S. T. Thompson, and C. E. Wieman, *Phys. Rev. Lett.* **96**, 170401 (2006).
- [15] A. L. Marchant, T. P. Billam, T. P. Wiles, M. M. H. Yu, S. A. Gardiner, and S. L. Cornish, *Nat. Commun.* **4**, 1865 (2013).
- [16] G. D. McDonald, C. C. N. Kuhn, K. S. Hardman, S. Bennetts, P. J. Everitt, P. A. Altin, J. E. Debs, J. D. Close, and N. P. Robins, *Phys. Rev. Lett.* **113**, 013002 (2014).
- [17] J. L. Helm, T. P. Billam, and S. A. Gardiner, *Phys. Rev. A* **85**, 053621 (2012).
- [18] A. D. Martin and J. Ruostekoski, *New J. Phys.* **14**, 043040 (2012).
- [19] J. Cuevas, P. G. Kevrekidis, B. A. Malomed, P. Dyke, and R. G. Hulet, *New J. Phys.* **15**, 063006 (2013).
- [20] J. Polo and V. Ahufinger, *Phys. Rev. A* **88**, 053628 (2013).
- [21] J. L. Helm, S. J. Rooney, C. Weiss, and S. A. Gardiner, *Phys. Rev. A* **89**, 033610 (2014).
- [22] J. L. Helm, S. L. Cornish, and S. A. Gardiner, *Phys. Rev. Lett.* **114**, 134101 (2015).
- [23] N. G. Parker, A. M. Martin, S. L. Cornish, and C. S. Adams, *J. Phys. B: At. Mol. Opt. Phys.* **41**, 045303 (2008).
- [24] J. H. V. Nguyen, P. Dyke, D. Luo, B. A. Malomed, and R. G. Hulet, *Nature Physics* **10**, 918 (2014).
- [25] C. Weiss and Y. Castin, *Phys. Rev. Lett.* **102**, 010403 (2009).
- [26] A. I. Streltsov, O. E. Alon, and L. S. Cederbaum, *Phys. Rev. A* **80**, 043616 (2009).
- [27] B. Gertjerenken, T. P. Billam, L. Khaykovich, and C. Weiss, *Phys. Rev. A* **86**, 033608 (2012).
- [28] C. Lee and J. Brand, *EPL (Europhysics Letters)* **73**, 321 (2006).
- [29] T. Ernst and J. Brand, *Phys. Rev. A* **81**, 033614 (2010).
- [30] A. L. Marchant, S. Händel, S. A. Hopkins, T. P. Wiles, and S. L. Cornish, *Phys. Rev. A* **85**, 053647 (2012).
- [31] N. R. Claussen, S. J. J. M. F. Kokkelmans, S. T. Thompson, E. A. Donley, E. Hodby, and C. E. Wieman, *Phys. Rev. A* **67**, 060701 (2003).
- [32] P. A. Ruprecht, M. J. Holland, K. Burnett, and M. Edwards, *Phys. Rev. A* **51**, 4704 (1995).
- [33] J. L. Roberts, N. R. Claussen, S. L. Cornish, E. A. Donley, E. A. Cornell, and C. E. Wieman, *Phys. Rev. Lett.* **86**, 4211 (2001).
- [34] E. A. Donley, N. R. Claussen, S. L. Cornish, J. L. Roberts, E. A. Cornell, and C. E. Wieman, *Nature (London)* **412**, 295 (2001).
- [35] D. Jenkin, D. McCarron, M. Köppinger, H. Cho, S. Hopkins, and S. Cornish, *The European Physical Journal D* **65**, 11 (2011).
- [36] The magnetic gradient required to levitate ^{85}Rb atoms in the $F = 2, m_F = -2$ state is $B'_z = 22.5 \text{ G cm}^{-1}$, however, it is found to be beneficial during evaporation to reduce the gradient slightly, to $B'_z \approx 21.5 \text{ G cm}^{-1}$ to allow atoms to be removed from the trap more easily.
- [37] Y.-J. Lin, A. R. Perry, R. L. Compton, I. B. Spielman, and J. V. Porto, *Phys. Rev. A* **79**, 063631 (2009).
- [38] Pixel values from shots with no atoms present are subtracted from the images to normalise the background noise level. This can lead to some reflection values below 0 %, however, the error bars associated with this calculation means these values are still consistent with zero.
- [39] L. D. Landau and E. M. Lifshitz, *Quantum mechanics: Non-relativistic Theory*, 3rd ed., Course of theoretical physics, Vol. 3 (Butterworth-Heinemann, Oxford, 1977) §25.
- [40] M. Born and E. Wolf, *Principles of Optics*, 4th ed. (Pergamon Press, Oxford, 1970).
- [41] C. M. Fabre, P. Cheiney, G. L. Gattobigio, F. Vermersch, S. Faure, R. Mathevet, T. Lahaye, and D. Guéry-Odelin, *Phys. Rev. Lett.* **107**, 230401 (2011).
- [42] S. L. Cornish, N. G. Parker, A. M. Martin, T. E. Judd, R. G. Scott, T. M. Fromhold, and C. S. Adams, *Physica D* **238**, 1299 (2009).
- [43] A. L. Marchant, T. P. Billam, M. M. H. Yu, A. Rakonjac, J. L. Helm, J. Polo, C. Weiss, S. A. Gardiner, and S. L. Cornish, “Quantum reflection of bright solitary matter-waves from a narrow attractive potential: Supporting data,” [dx.doi.org/10.15128/cc24b379-1be2-4c42-862b-8895aa495968](https://doi.org/10.15128/cc24b379-1be2-4c42-862b-8895aa495968) (2015).